ENERGETIC PARTICLE INSTABILITIES IN FUSION PLASMAS

S.E.Sharapov[1], B.Alper[1], H.L.Berk[2], D.N.Borba[3], B.N.Breizman[2], C.D.Challis[1], I.G.J.Classen[4], E.M.Edlund[5], J.Eriksson[6], A.Fasoli[7], E.D.Fredrickson[5], G.Y.Fu[5], M.Garcia-Munoz[8], T.Gassner[9], K.Ghantous[5], V.Goloborodko[9], N.N.Gorelenkov[5], M.P.Gryaznevich[1], S.Hacquin[10], W.W.Heidbrink[11], C.Hellesen[6], V.G.Kiptily[1], G.J.Kramer[5], P.Lauber[8], M.K.Lilley[12], M.Lisak[13], F.Nabais[3], R.Nazikian[5], R.Nyqvist[13], M.Osakabe[14], C.Perez von Thun[8,15], S.D.Pinches[16], M.Podesta[5], M.Porkolab[17], K.Shinohara[18], K.Schoepf[9], Y.Todo[14], K.Toi[14], M.A.Van Zeeland[19], I.Voitsekhovich[1], R.B.White[5], V.Yavorskij[9], ITPA EP TG, JET-EFDA Contributors[*]

JET-EFDA, Culham Science Centre, Abingdon, OX14 3DB, UK

[1]Euratom/CCFE Fusion Association, Culham Science Centre, Abingdon, OX14 3DB, UK

[2]Institute for Fusion Studies, University of Texas at Austin, Austin, Texas 78712, USA

[3]Assoc. EURATOM/IST, Inst. de Plasmas e Fusão Nuclear - IST, UTL, P-1049-001 Lisboa, Portugal

[4]FOM institute DIFFER – Assoc. Euratom-FOM, Nieuwegein, The Netherlands

[5]Princeton Plasma Physics Laboratory, Princeton NJ 08543, USA

[6]Dept. Physics & Astronomy, Uppsala University, Euratom/VR Fusion Assoc., Uppsala, Sweden

[7]CRPP/EPFL, Association Euratom-Confederation Suisse, Lausanne, Switzerland

[8]Max Planck Institute für Plasmaphys., Euratom Assoc., Boltsmannstr.2, Garching, Germany

[9]Euratom/OEAW Fusion Assoc., Inst. Theoretical Physics, Univ. of Innsbruck, A-6020, Austria

[10]CEA, IRFM, Assoc. Euratom-CEA, St Paul Lez Durance, France

[11]Dept. of Physics and Astronomy, University of California, Irvine, CA 92697, USA

[12]Physics Department, Imperial College, London, SW7 2AZ, UK

[13]Dep. of Earth and Space Science, Chalmers Univ. of Technology, Goteborg, Sweden

[14]National Institute for Fusion Science, 322-6 Oroshi-cho, Toki 509-5292, Japan

[15]JET-EFDA Close Support Unit, Culham Science Centre, Abingdon, OX14 3DB, UK

[16]ITER Organization, Route de Vinon sur Verdon, 13115 St Paul-lez-Durance, France

[17]Plasma Science and Fusion Centre, MIT, Cambridge, Massachusetts 02139, USA

[18]Japan Atomic Energy Agency, Naka, Ibaraki 319-0193, Japan

[19]General Atomics, San Diego, CA 92186-5608, USA

***See the Appendix of F. Romanelli et al., Proc. 24th IAEA Fusion Energy Conference 2012, San Diego, USA**

Outline

- Introduction
- Recent advances in diagnosing Alfvén instabilities
- Redistribution of energetic ions caused by Alfvén instabilities: experiment and modelling
- The near-threshold nonlinear theory of frequency sweeping modes
- Possible control of Alfvén instabilities in burning plasmas using ECRH
- Summary

Introduction

Energetic particle (EP) driven instabilities in magnetic fusion

- **Present day machines with energetic particles reveal EP instabilities in a broad frequency range: fishbones, EGAMs, BAEs, AEs, EPMs, CAEs, etc. (see, e.g. [*] and References therein).**

- **Among these, weakly-damped Alfvén eigenmodes (AEs) are the top priority for α-particles in ITER since**

1. **AEs are driven by radial gradient of α-particle pressure (in contrast to, e.g., CAEs driven by velocity gradients)**
2. **AEs in ITER will resonate with α-particles in the MeV range (in contrast to, e.g. fishbones resonating with α-particles of 300-400 keV)**
3. **Due to its weak damping, AEs could be excited by α-particle population with low energy content per volume (in contrast to EPMs)**

- **The weakly damped AEs have been extensively researched and they now provide one of the best cases for detailed theory-experiment comparisons, which is the focus of this overview.**

[*] BREIZMAN B.N., SHARAPOV S.E. 2011 Plasma Phys. Control. Fusion 53 054001

Energetic particle driven AE instabilities

- For typical burning DT plasmas, α-particles born at 3.5 MeV are super-Alfvénic:

$$V_{Ti} << V_A \leq V_\alpha << V_{Te},$$

  and may excite AE instability via $V_{||\alpha} = V_A$ resonance, where $V_A = B/(4\pi \Sigma_i n_i M_i)^{1/2}$

- AE instability can cause a significant radial re-distribution of α-particles with a minor change in their energy → less favourable α-heating profiles and excessive loss of α-particles [1]

- Existence of stable AEs and their weak damping were studied extensively with external AE antennae [1]

- AE instabilities driven by α-particles were first seen on TFTR [2]

- AE instabilities reveal two main scenarios, with mode frequency locked (FL) to the plasma equilibrium and with mode frequency sweeping (FS)

[1] FASOLI A., GORMEZANO C., BERK H.L., et al. 2007 Nucl. Fusion 47 S264
[2] NAZIKIAN R., et al. 1997 Phys. Rev. Lett. 78 2976

Alfvén instabilities with frequency locked (FL) to plasma equilibrium and with frequency sweeping (FS)

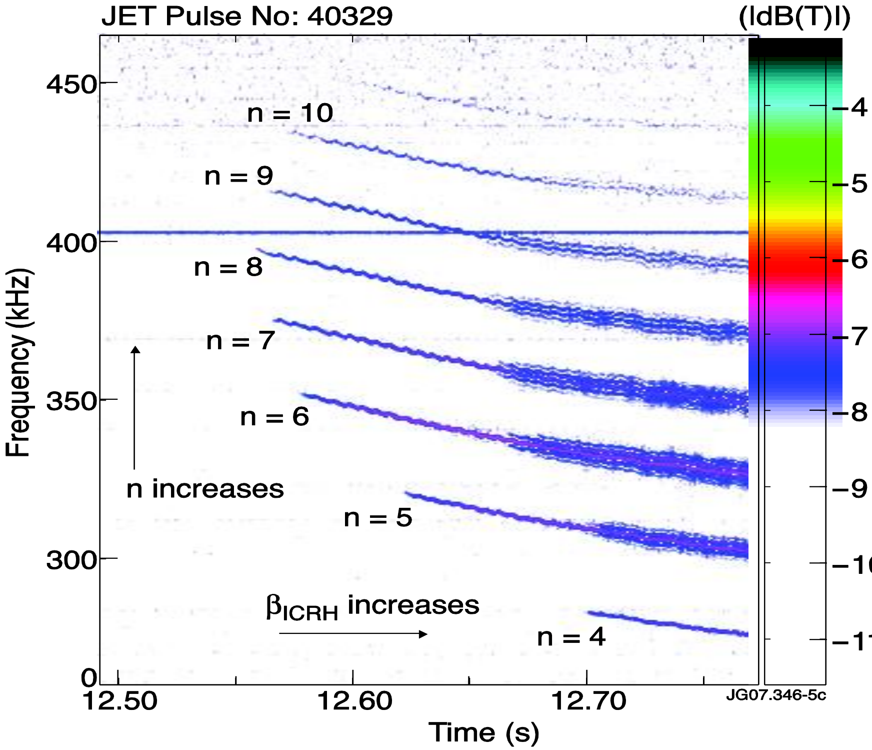

FIG.1 JET: ICRH-driven TAEs have frequencies following equilibrium changes in accordance with $V_A \sim B/n^{1/2}$ scaling [3]

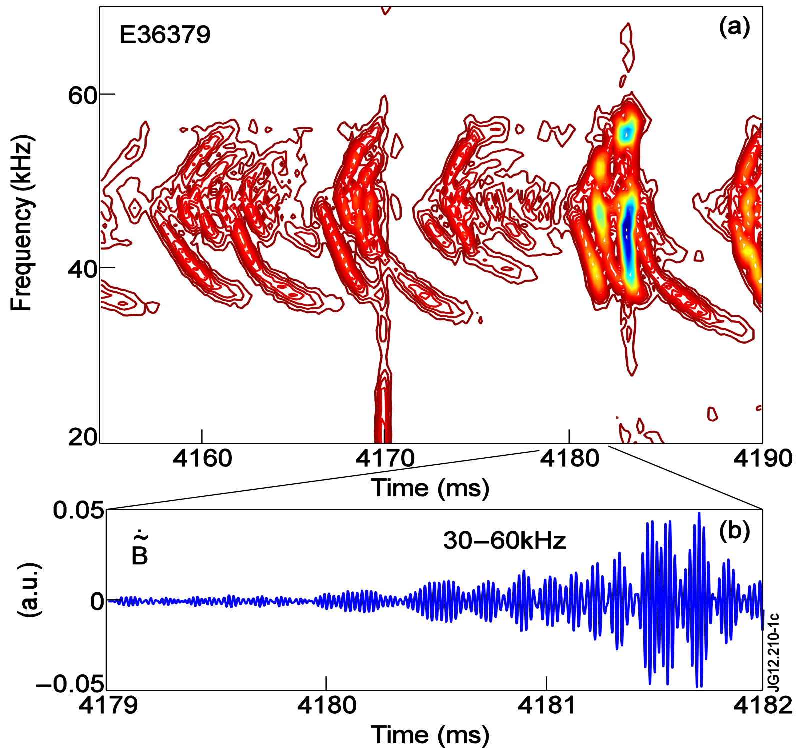

FIG.2 JT60U: (a) NBI-driven FS Alfvén instability start from TAE frequency, but sweeps away faster than equilibrium changes; b) Mirnov coil signal [4]

[3] KERNER W., BORBA D., SHARAPOV S.E., et al. 1998 Nucl. Fusion 38 1315

[4] SHINOHARA K., KUSAMA Y., TAKECHI M., et al. 2001 Nucl. Fusion 41 603

AE instabilities with frequency locked (FL) to equilibrium versus frequency sweeping (FS) instabilities

- **FL: frequency of unstable AE corresponds to linear AE determined by bulk plasma equilibrium. Re-distribution of energetic particles only saturates the growth rate but does not affect the AE frequency**

- **FS scenario: contribution of the energetic particles to mode frequency is as essential as the bulk plasma contribution. When the unstable mode re-distributes the energetic particles, it changes the frequency too**

- **The FL and FS scenarios differ in temporal evolution and in the type of transport (diffusive for FL and mostly convective for FS)**

Advances in diagnosing Alfvén instabilities

Search for techniques of investigating AEs in the plasma core

- **Magnetic sensors outside plasma may not detect AEs in the plasma core (δB_{edge} measurement)**
- **Future DT machines like DEMO will have a restricted access to plasma → we should look for AE detection tools naturally combined with other diagnostics**
- **Possibilities of detecting AEs via δn and δT were explored and two techniques, interferometry [5] and ECE [6], were found to be suitable and robust**
- **Phase Contrast Imaging (PCI) [7], 2D ECE imaging (ECEI) [8,9], and beam emission spectroscopy [10] were developed for identifying the mode structure (in addition to X-mode reflectometry and SXR)**
- **These new techniques provide confidence that we can now detect all unstable modes**

[5] SHARAPOV S.E., ALPER B., FESSEY J., et al. 2004 Phys. Rev. Lett. 93 165001
[6] VAN ZEELAND M.A., KRAMER G.J., AUSTIN M.E., et al. 2006 Phys. Rev. Lett. 97 135001
[7] EDLUND E.M., PORKOLAB M., KRAMER G. J., et al. 2010 Plasma Phys. Control.Fusion 52 115003
[8] CLASSEN I.G.J., BOOM J.E., SUTTROP W., et al. 2010 Rev. Sci. Instr. 81 10D929
[9] TOBIAS B.J., et al. 2011 Phys. Rev. Lett. 106 075003
[10] DURST, R.D., et al. 1992 Phys. Fluids B4 3707

Interferometry detection of core-localised modes

- **Interferometry technique of detecting Alfvén instabilities via δn in the plasma core is often superior to magnetic sensors outside the plasma**

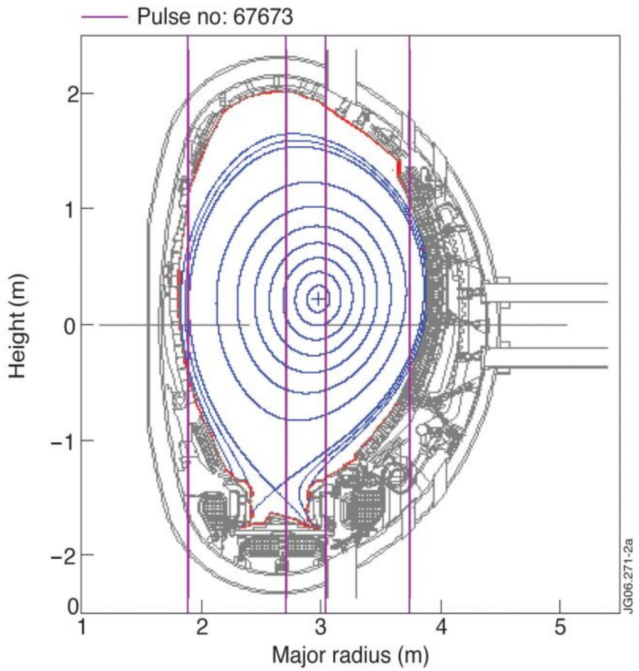

FIG.3 Geometry of JET FIR interferometer with vertical lines-of-sights

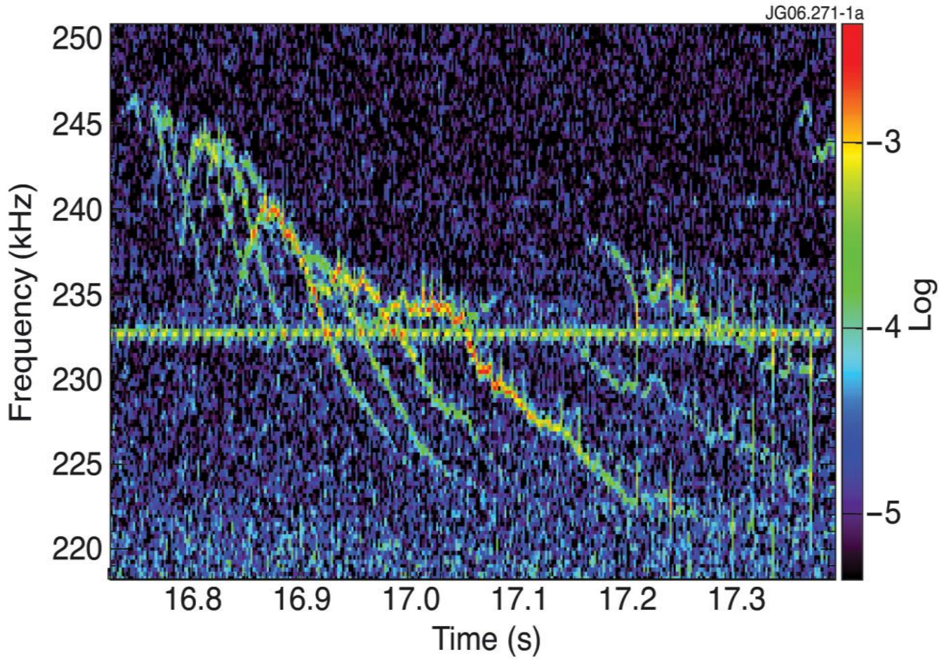

FIG.4 Core-localised TAEs detected with JET interferometer. Some of these TAEs are not seen on Mirnov coils.

ECE radial profiles on DIII-D versus ideal MHD modelling

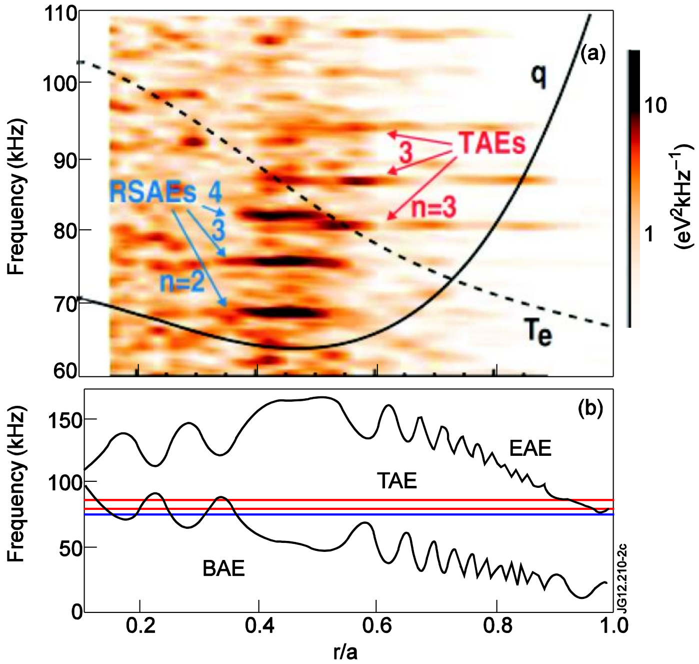

FIG.5 DIII-D discharge 122117: (a) Radial profile of ECE power spectra showing RSAEs and TAEs; (b) n = 3 Alfvén continuum [6].

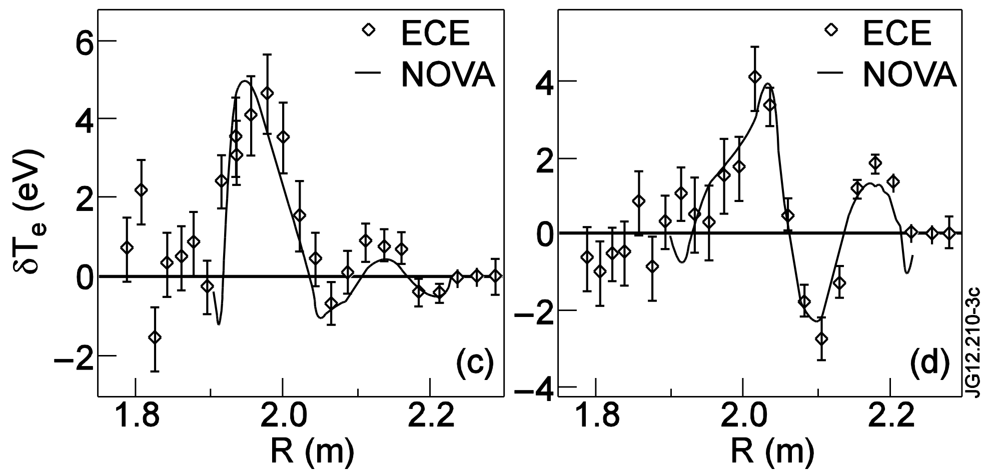

$\delta T_e / T_e \approx 0.5\%$

$\delta B / B \approx$ (1.5±0.14) 10^{-4} for RSAE

$\delta B / B \approx$ (2.5±0.18) 10^{-4} for TAE

FIG.6 DIII-D: Diamonds show ECE radiometer measured δT_e for RSAE (left) and TAE (right) from Figure 5; solid line shows the ideal MHD (NOVA code) predictions.

Redistribution and losses of energetic ions caused by FL Alfvén instabilities

What energetic particles are redistributed?

AE mostly affects particles in narrow region of phase space satisfying the wave-particle resonance condition:

$$\Omega \equiv \omega - n\omega_{\varphi}\left(E,\ P_{\varphi},\ \mu\right) - l\omega_{\vartheta}\left(E,\ P_{\varphi},\ \mu\right) = 0$$

where $l = 0,\ \pm 1, \ldots$, **and toroidal** $\omega_{\varphi}\left(E,\ P_{\varphi},\ \mu\right)$ **and poloidal** $\omega_{\vartheta}\left(E,\ P_{\varphi},\ \mu\right)$ **orbit frequencies of the particles in the unperturbed field are functions of energy** E**, magnetic moment** μ **and toroidal canonical angular momentum** P_{φ}

In the nonlinear phase of the instability, the resonant particles can become trapped in the field of the wave within a finite width of the resonance,

$$\Delta\Omega \cong \omega_{NL}$$

where ω_{NL} **is the nonlinear trapping frequency**

If the widths of different resonances are smaller than the distance between them, a single mode nonlinear theory applies. If the resonances overlap, stochastic diffusion of the particles over the resonances can cause a global transport [11,12]

[11] BERK H.L., BREIZMAN B.N., PEKKER M.S. 1995 Nucl. Fusion 35 1713
[12] WHITE R.B., CHANCE M.S. 1984 Phys. Fluids 27 2455

JET: TAEs inside the q=1 radius re-distribute ICRH-accelerated beam ions [13]

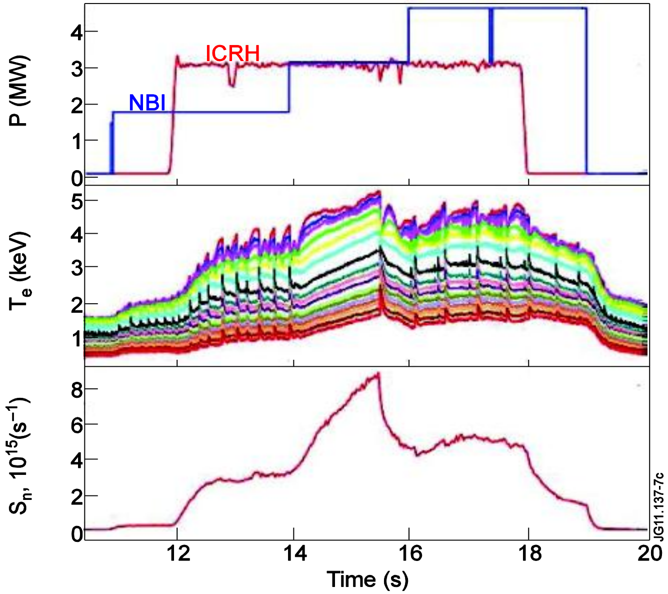

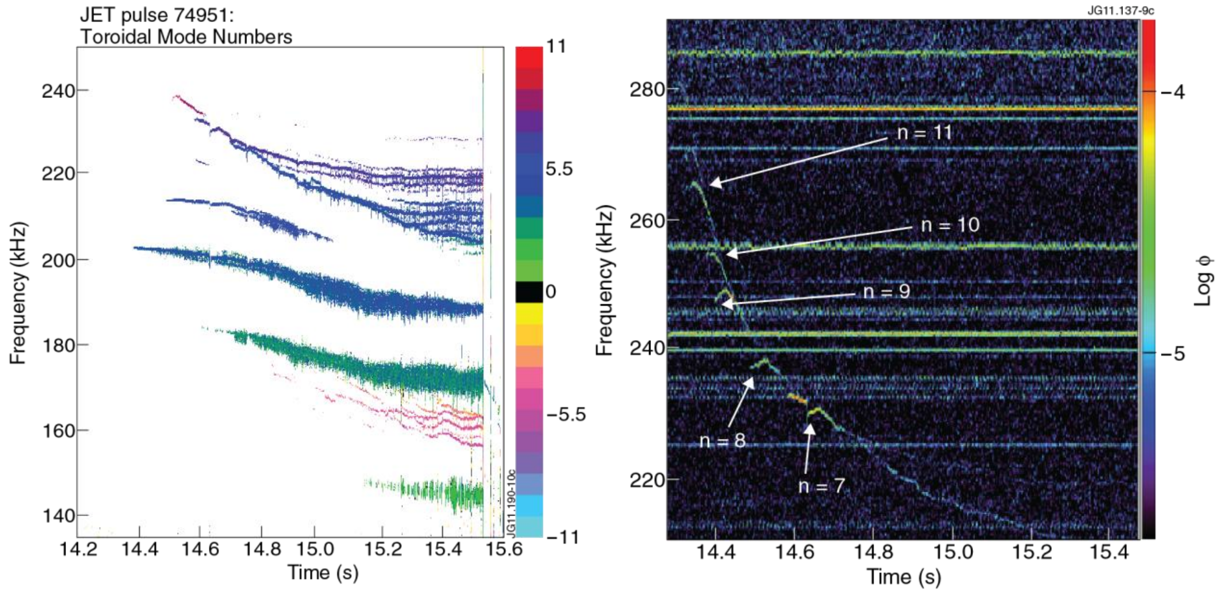

Mirnov coils ***FIR interferometry***

FIG.5 Top: P_{NBI} and P_{ICRH} in JET discharge #74951. Middle: T_e measured with multi-channel ECE. Bottom: DD neutron yield.

FIG.6 TAEs detected with Mirnov coils (left) and core-localised TAE inside q=1 (tornado modes) detected with FIR interferometry (rigjt) in JET discharge # 74951.

[13] GASSNER T., SCHOEPF K., SHARAPOV S.E., et al. 2012 Phys. of Plasmas 19 032115

Redistribution of the energetic ions during the TAE activity

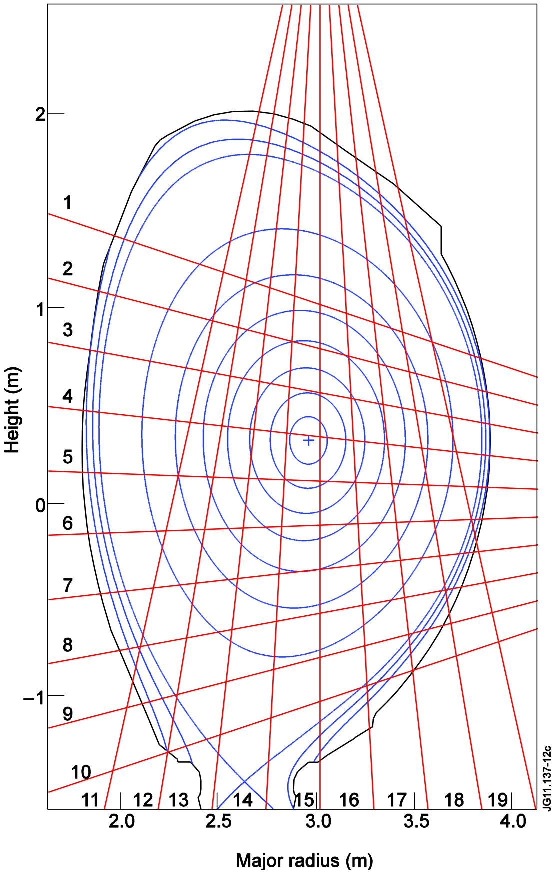

FIG.7 Lines-of-sights of the 2D gamma-camera on JET.

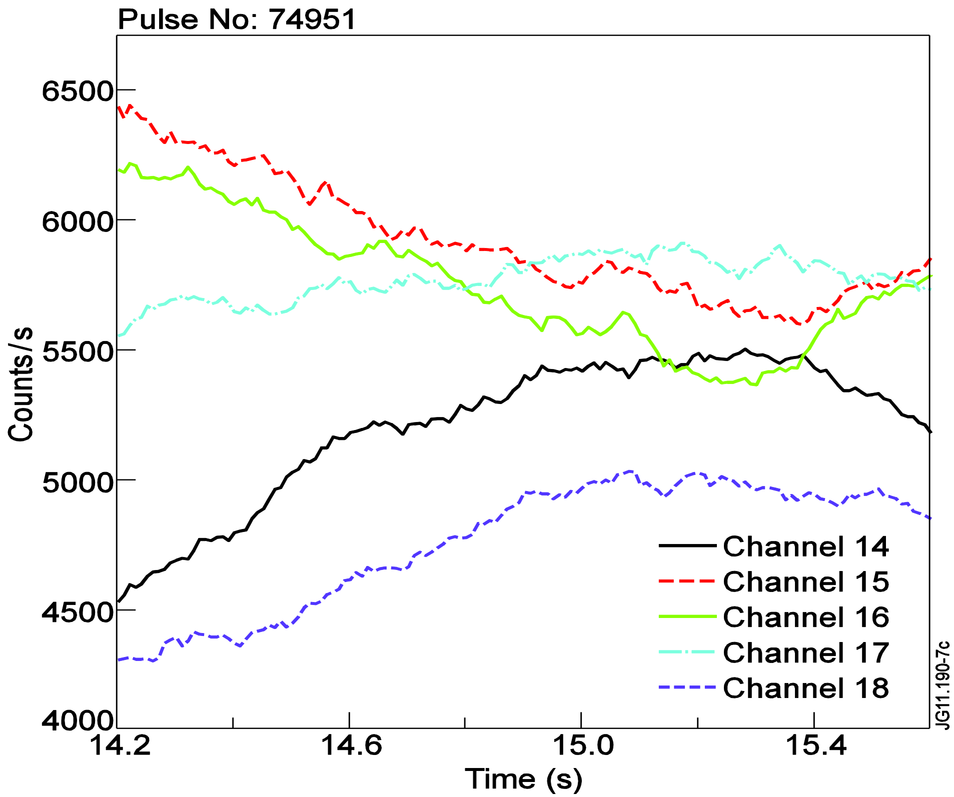

FIG.8 Time evolution of γ-ray intensity from $^{12}C(D,p)^{13}C$ reaction involving D ions with E>500 keV in JET discharge # 74951. The signals in central channels (15, 16) decrease, while the signals in outer channels (14,18) increase.

Modelling of TAE-induced redistribution of energetic ions

- **Guiding centre codes like HAGIS [14] or ORBIT [12] can be used to compute energetic particle interaction with AEs**
- **HAGIS/ORBIT approach is a necessary first step in modelling but the big challenge in prediction is knowing what amplitude the modes will obtain.**

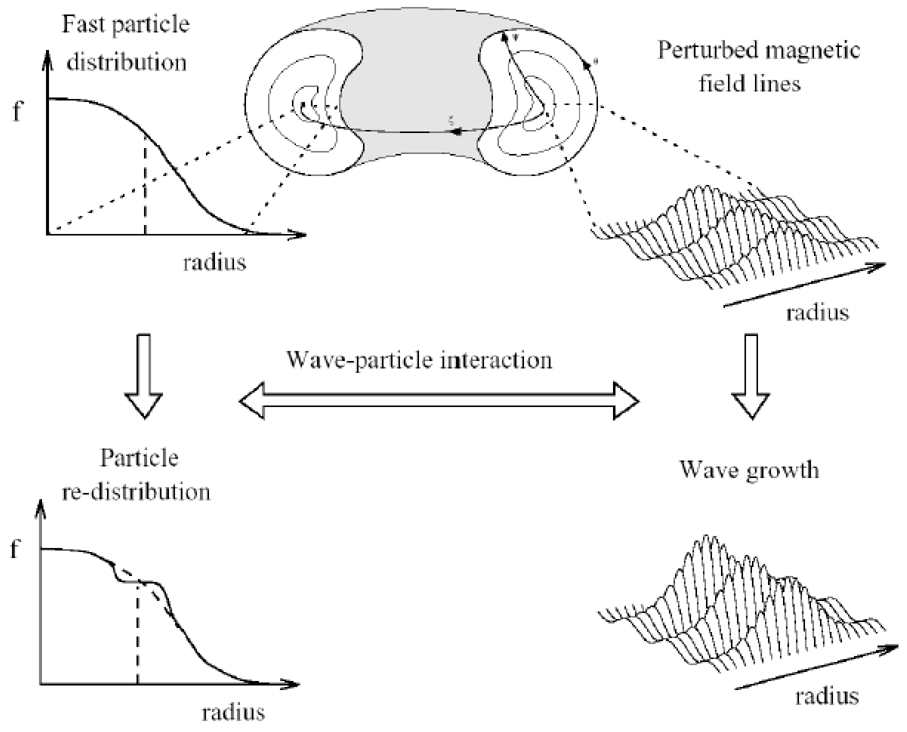

[14] PINCHES S.D., et al., 1998 Comp. Phys. Comm. 111 133

Modelling of TAE-induced redistribution of energetic ions with the initial value HAGIS code

- **The input at t=0 (before TAE excitation) consists of: reconstructed equilibrium, all AEs computed (ideal MHD code), and fast particle distribution in the form**

$$f(E,\ P_\varphi,\ \mu) = f(E)\cdot f(P_\varphi)\cdot f(\Lambda)$$

with $\Lambda \equiv \mu B_0 / E$ **and** $f(P_\varphi)$ **for trapped ions means radial profile** $f(\psi)$.

- $f(E)$ **is obtained from experimentally measured spectrum of DD neutrons [15]**
- **The radial profile** $f(\psi)$ **is obtained from experimentally measured 2D profile of γ-rays from nuclear** $^{12}C(D,p)^{13}C$ **reaction [16]**
- **For D beam ions accelerated with on-axis ICRH,** $f(\Lambda)$ **is taken as Gaussian centred at** $\Lambda = 1$ **with the width** $\Delta\Lambda = 1.5\cdot 10^{-1}$
- **The HAGIS run for the coupled AEs + energetic ions shows an exponential growth of the AEs followed by nonlinear saturation and redistribution of the ions**

[15] HELLESEN K., GATU JOHNSON M., ANDERSSON SUNDEN E., et al. 2010 Nucl. Fusion 50 084006
[16] KIPTILY V.G., CECIL F.E., JARVIS O.N., et al. 2002 Nucl. Fusion 42 999

TAE-induced redistribution of the energetic ions

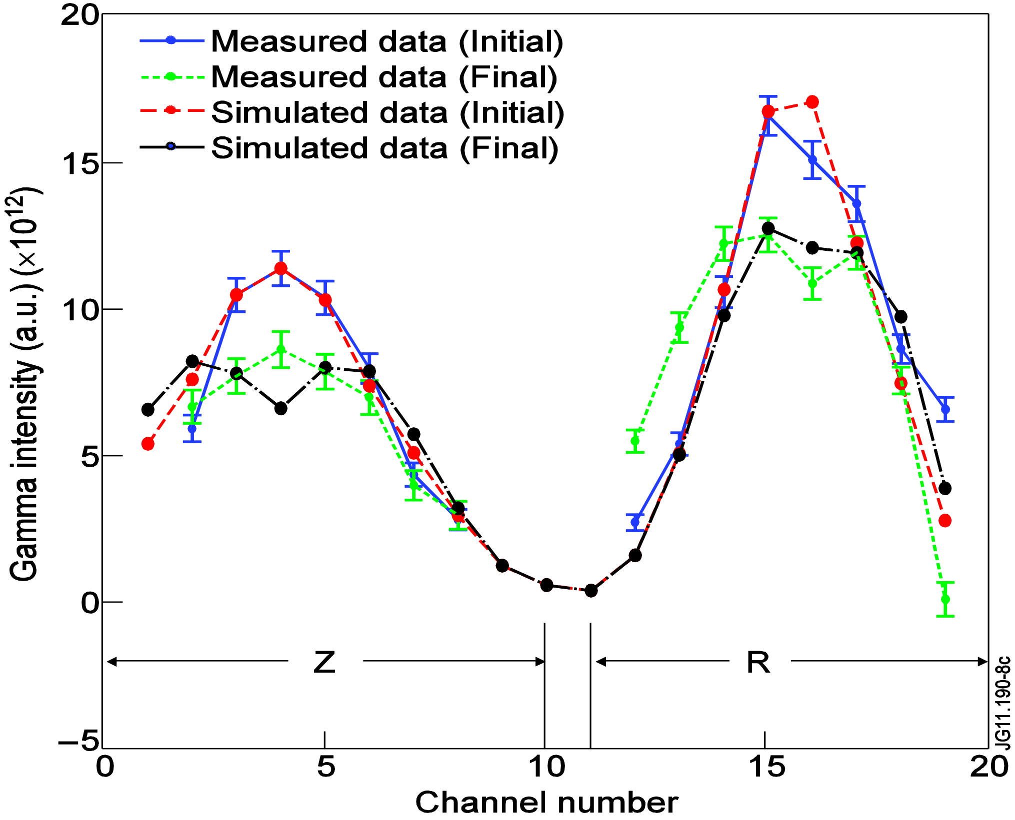

FIG.9 Intensity of γ-rays from energetic D ions in the 19 channels of gamma-camera (JET pulse # 74951). Here we show measured pre-TAE (blue) and during TAE (green) profiles. Simulated γ-intensity is shown in red (initial data) and black (after redistribution) [13].

DIII-D: strong flattening of beam ion profile is observed in reversed-shear discharges with Alfvén instabilities [17]

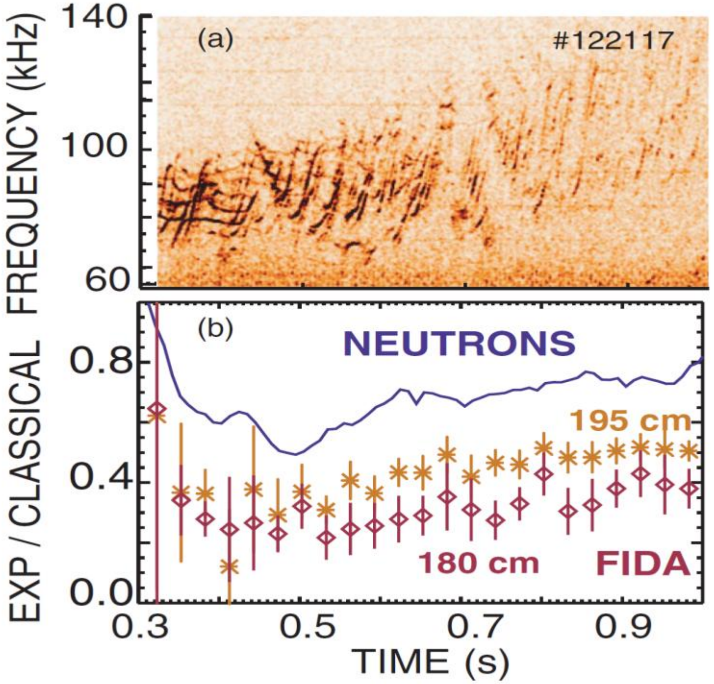

FIG.10 (a) interferometer spectrogram showing AEs; (b) Neutron rate and FIDA densities. The signals are normalized by the classical TRANSP predictions.

[17] HEIDBRINK W.W., et al. 2007 Phys. Rev. Lett 2007 99 245002

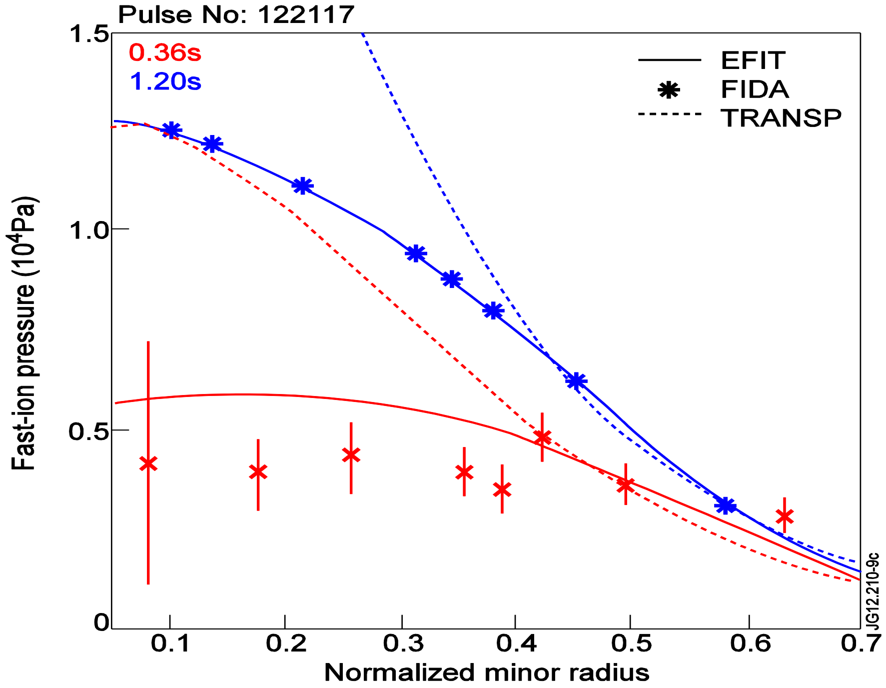

FIG.11 p_f profiles and FIDA density profiles at 0.36 s and 1.2 s corresponding to normalized neutron rates of 0.66 and 0.94. The dashed lines are the profiles predicted by TRANSP. The FIDA density profile is normalized to the MSE-EFIT p_f profile at 1.2 s.

ORBIT modelling explains the global flattening by stochastic diffusion across many overlapped resonances [18]

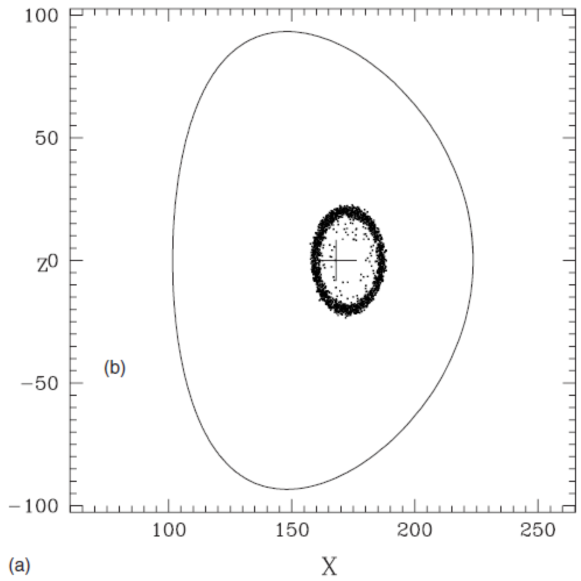

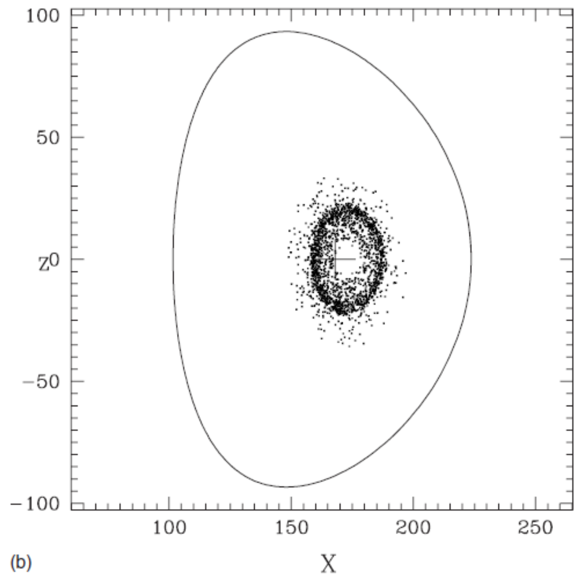

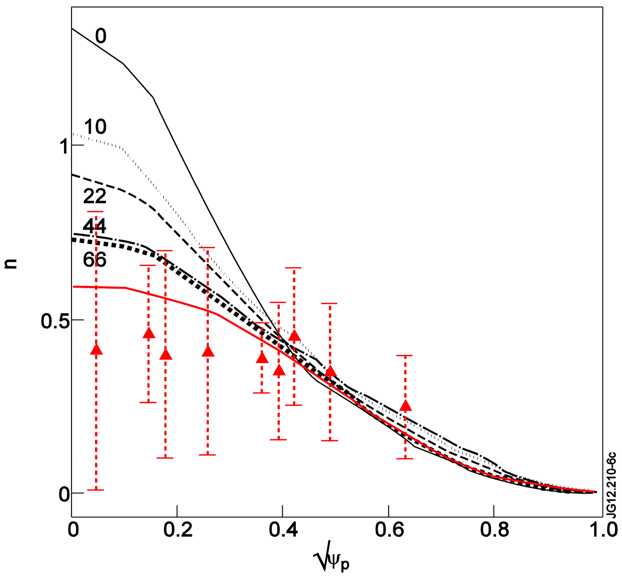

$\delta B/B$=1.2x10^{-4} ***$\delta B/B$=1.6x10^{-4}***

FIG.12 ORBIT: Beam distribution after 7 ms in the presence of the full spectrum of modes, but with no collisions.

FIG.13 Radial profiles of the beam ions from the ORBIT code with AEs (black) compared with data (red).

[18] WHITE R.B., GORELENKOV N., HEIDBRINK W., VAN ZEELAND M. 2010 Phys. Plasmas 17 056107

The near-threshold nonlinear theory of frequency sweeping modes

Hard and soft mode excitation near the threshold

- **The near-threshold condition reads** $\gamma \equiv \gamma_L - \gamma_d << \gamma_d \le \gamma_L$
- **In this limit, a lowest order cubic nonlinear equation for bump-on-tail gives equation for temporal evolution of the wave amplitude $A(t)$ [19,20]:**

$$\frac{dA}{d\tau} = A(\tau) - \frac{1}{2}\int_0^{\tau/2} dz\ z^2 A(\tau - z)\int_0^{\tau-2z} dx\ \exp\left[-\nu^3 z^2\left(\frac{2z}{3} + x\right) - \beta(2z + x)\right]\cdot \exp\left[i\alpha^2 z(z + x)\right] \times A(\tau - z - x)A^*(\tau - 2z - x),$$

$$\tau \equiv (\gamma_L - \gamma_d)t$$

showing that the sign in front of the nonlinear term can change depending on the type of relaxation restoring the unstable distribution function, diffusion (term with ν) or drag (term with α). For pure drag, only explosive solutions exist without steady-state.

[19] BERK H.L., BREIZMAN B.N., PEKKER M.S. 1996 Phys. Rev. Lett. 76 1256
[20] LILLEY M.K., BREIZMAN B.N., SHARAPOV S.E. 2009 Phys. Rev. Lett. 102 195003

Fully nonlinear model of the "hard" excitation

- Beyond the cubic nonlinearity, a fully nonlinear model shows formation of long-living structures, holes and clumps, in distribution function [21,22]
- These structures move in phase space changing the frequency of initial perturbation [23]

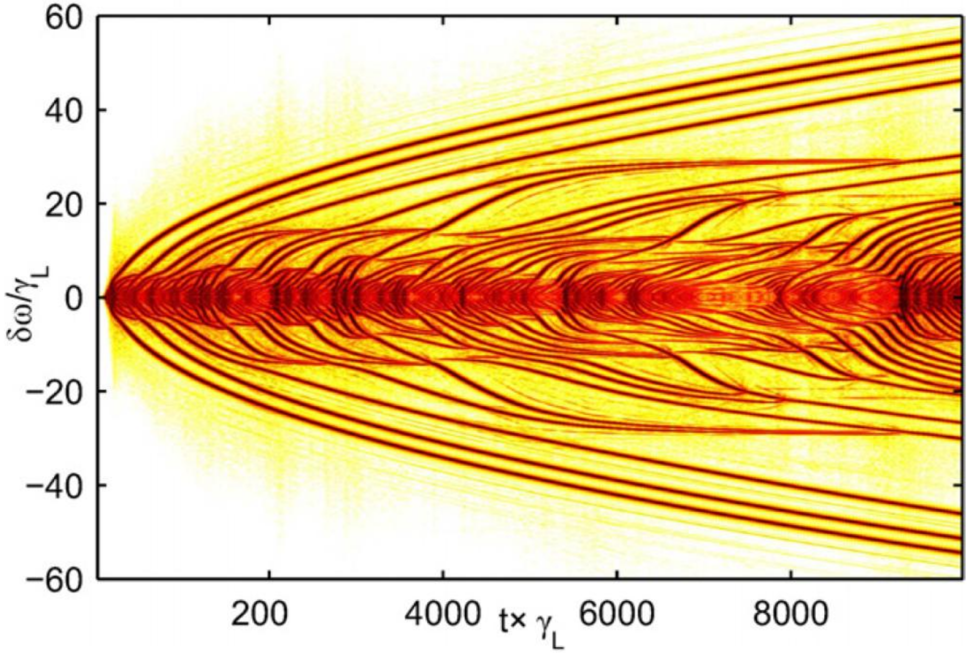

[21] BERK H.L., BREIZMAN B.N., PETVIASHVILI N.V.1997 Phys. Lett. A234 213
[22] LILLEY M.K., BREIZMAN B.N., SHARAPOV S.E. 2010 Phys. Plasmas 17 092305
[23] BREIZMAN B.N. 2010 Nucl. Fusion 50 084014

Experimental detection of holes and clumps with NPA on LHD [24]

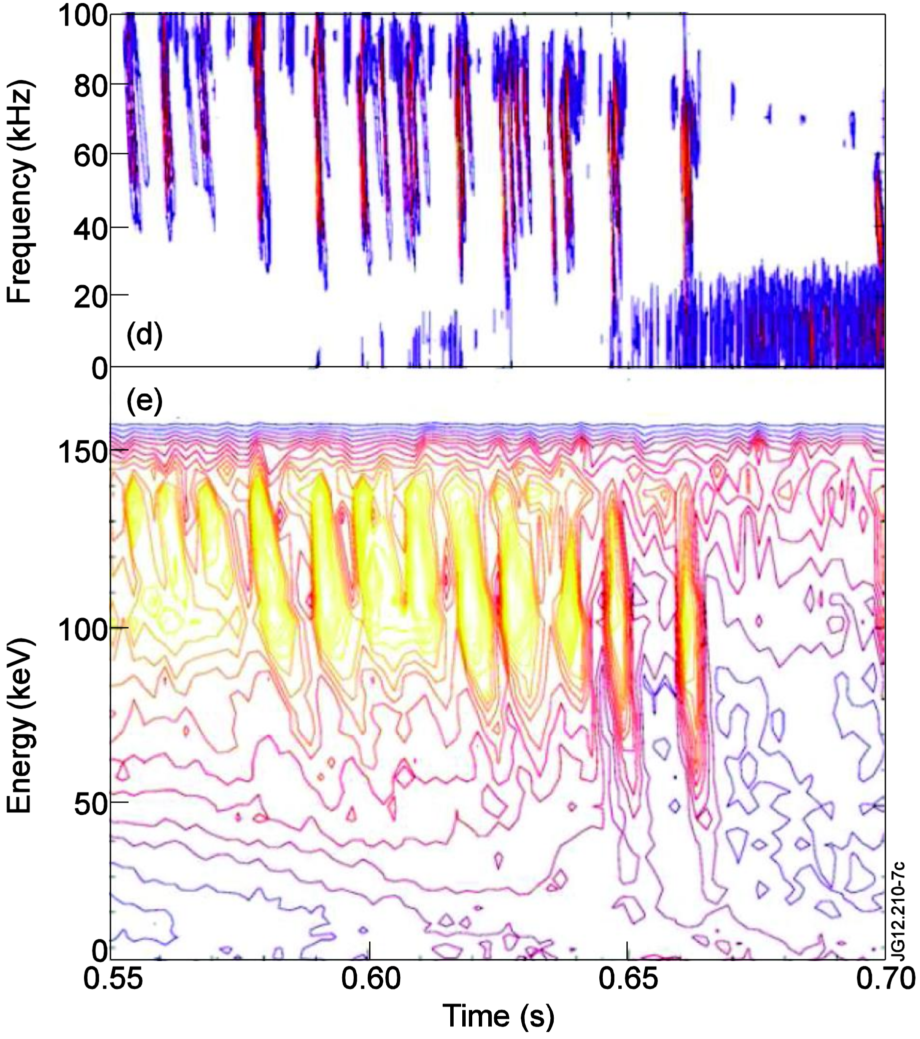

Search for the long-living nonlinear structures in energetic ion distribution was performed for validating the theory

Figure 15. Top: magnetic spectrogram of NBI-driven AEs; Bottom: Time evolution of tangential energetic neutral spectrum measured with NPA (viewing angle is set to 0^0) .

[24] OSAKABE M., YAMAMOTO M., TOI K., et al. 2006 Nucl. Fusion 46 S911

Frequency sweeping modes: experiment and modelling in real tokamak geometry

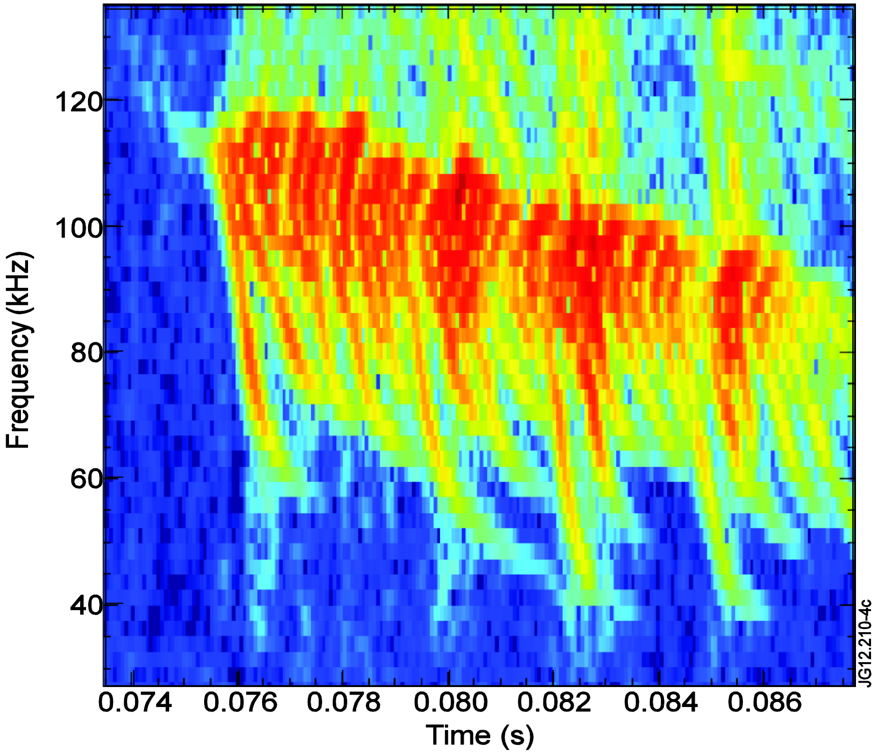

FIG.16 Magnetic spectrogram showing FS Alfvén modes driven by NBI in MAST discharge #27177.

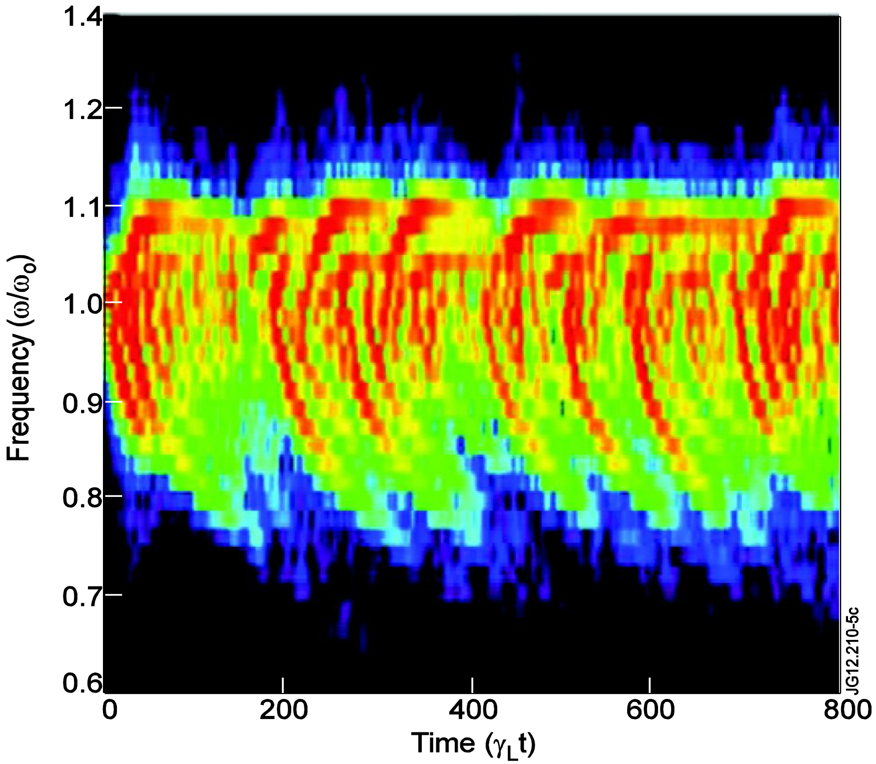

FIG.17 Nonlinear HAGIS simulation of TAE with unlocked phase driven by slowing-down beam distribution function.

Possible control of Alfvén instabilities in burning plasmas using ECRH

Suppression of Alfvénic activity with ECRH on DIII-D [25]

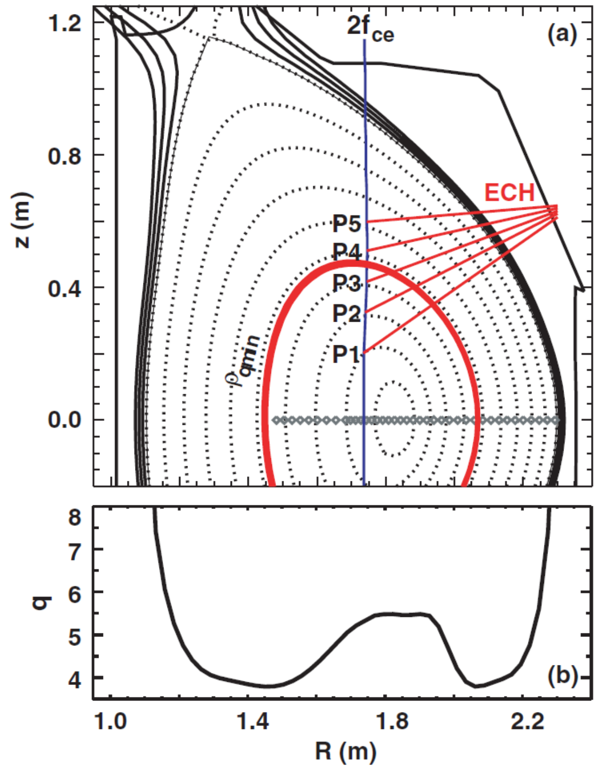

FIG.18 (a) DIII-D equilibrium showing $2f_{ce}$ location (blue), ECH deposition locations (P1-P5), ECE radiometer channel locations (gray diamonds) and q_{min} surface (red); (b) q-profile

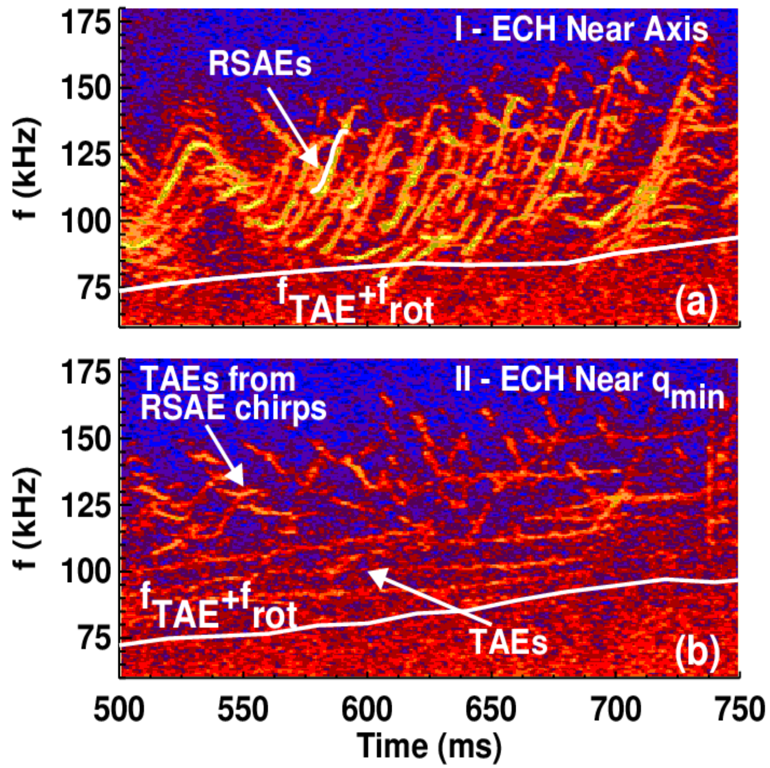

FIG.19 Spectra of vertical and radial CO_2 interferometer data for 1.9MW ECRH deposition at (a) near axis in #128564, (b) near q_{min} in #128560.

[25] VAN ZEELAND M.A., HEIDBRINK W., NAZIKIAN R., et al. 2008 PPCF 50 035009

Suppression of Alfvénic activity with ECRH on ITER - ?

- **On ITER, global high-n (n>10) TAEs are expected to be most unstable.**

- **ECRH may be applied in a prescribed narrow region in order to form a TAE-free transport barrier preventing radial transport of alpha-particles**

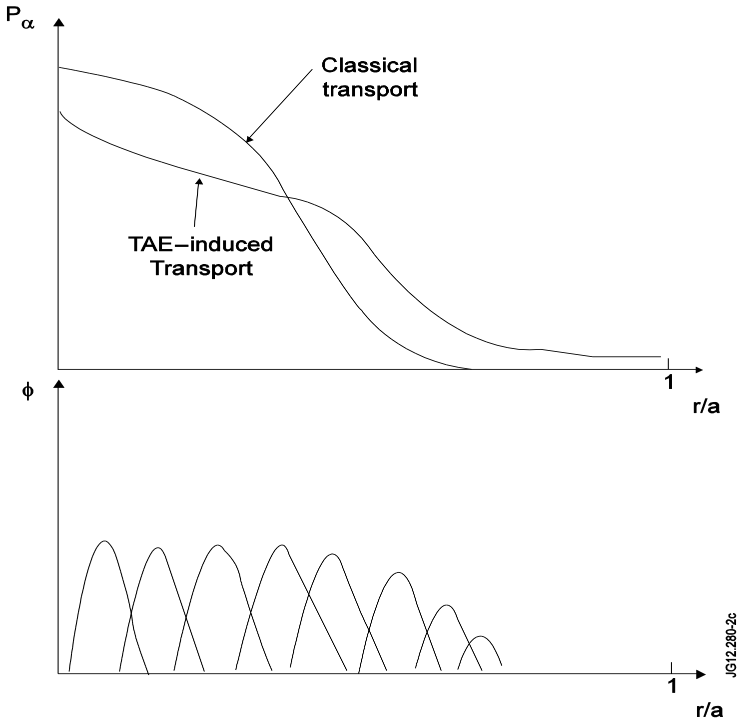

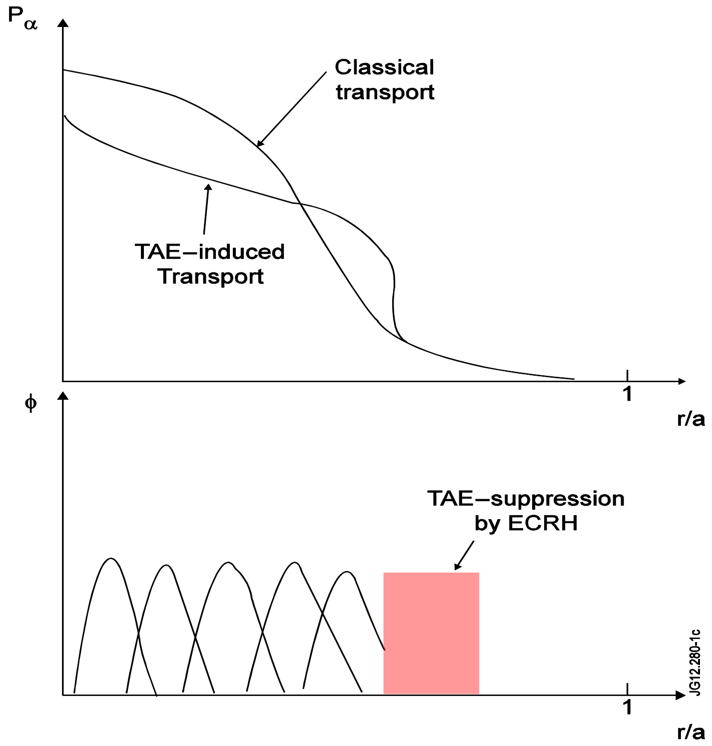

Summary

- **Recently developed techniques of diagnosing EP-driven Alfvén instabilities with interferometry, ECE, phase contrast imaging, and beam emission spectroscopy set a stage for new understanding of such instabilities relevant to burning plasma**

- **Theory-to-experiment comparison of AE-induced redistribution of energetic particles shows satisfactory agreement for well-diagnosed instabilities with wave-particle resonances non-overlapped and overlapped, for $\rho_{HOT}/a \sim 0.1$**

- **Near-threshold fully nonlinear theory displays many characteristics of Alfvénic modes with frequency sweeping seen in experiments**

- **ECRH suppression of AE activity on DIII-D encourages development of techniques allowing control over AEs on ITER**

Presentations on energetic particles at this Conference:

Experimental study of energetic particle-driven Alfvén instabilities:

EX/P6-05 Fredrickson, Eric USA Fast-ion Energy Loss during TAE Avalanches in the National Spherical Torus Experiment
EX/5-1 Matsunaga, Go Japan Dynamics of Energetic Particle Driven Modes and MHD Modes in Wall-stabilized…
EX/5-2 Yamamoto, Satoshi Japan Studies of Energetic-ion-driven MHD Instabilities in Helical Plasmas
EX/P6-09 Hole, Matthew Australia Analysis of Alfven Wave Activity in KSTAR Plasmas
EX/P6-13 Liu, Yi China Nonlinear features of the Alfvenic wave-particle interaction in auxiliary heated HL-2A plasma
EX/P6-23 Blackwell, Boyd Australia MHD Activity in the Alfven Range of Frequencies in the H-1NF Heliac
EX/P6-22 Heidbrink, William USA Fast Ion Physics Enabled by Off-Axis Neutral Beam Injection
EX/P6-28 Fasoli, Ambrogio Switzerland Basic Investigations of Electrostatic Turbulence and its Interaction with…
EX/P8-10 Nagasaki, Kazunobu Japan Stabilization of Energetic-Ion-Driven MHD Mode by ECCD in Heliotron J

Modelling:

TH/P3-34 Pinches, Simon UK Development of a Predictive Capability for Fast Ion Behaviour in MAST
TH/4-2 Zonca, Fulvio Italy Nonlinear Excitations of Zonal Structures by Toroidal Alfven Eigenmodes
TH/P6-19 Spong, Donald USA Application and Development of the Gyro-Landau Fluid Model for Energetic-particle…
TH/P6-22 Fu, Guo Yong USA Nonlinear Simulations of Beam-driven …
TH/P6-23 Chen, Liu China Nonlinear Studies of beta-Induced AE Driven by Energetic Particles in Fusion Plasmas

Frequency Sweeping energetic particle driven instabilities:

TH/4-1 Berk, Herbert USA Energetic Particle Long Range Frequency Sweeping and Quasilinear Relaxation
TH/P6-14 Lesur, Maxime Korea, Rep. Subcritical Growth of Coherent Phase-space Structures
TH/P6-20 Todo, Yasushi Japan Linear Properties and Frequency Chirping of Energetic Particle Driven …

Other: **TH/P3-35, EX/5-3,EX/P6-02, EX/P6-07, EX/P6-11, EX/P6-12, EX/P6-14, EX/P6-15, ITR/P5-36, EX/P6-06, EX/P6-27, ITR/P1-32, ITR/P1-33, ITR/P1-34, TH/P6-03, TH/P2-15, TH/P4-11, EX/P6-03, TH/P6-13, TH/P3-32, TH/P6-04, TH/P6-06, TH/P6-09, TH/P6-10, TH/P6-16, TH/P6-17, TH/P6-21, TH/P6-30, TH/P6-01**